



# A COMPARISON OF SENSOR BASED AND SENSORLESS TECHNIQUE FOR SPEED CONTROL OF PMSM DRIVE

Gaurav Aggarwal

G.B. Pant university of Agriculture and Technology, Pantnagar (Uttarakhand)

## Abstract

**This paper presents the comparison between sensor based and sensorless zero direct axis current control for permanent magnet synchronous motor (PMSM). Zero direct axis current control is used for speed control of PMSM for below base speed. Rotor position estimation has also been estimated by the use of back electromotive force (emf) space vector for permanent magnet synchronous motor. Sensorless technique is more reliable and preferable over sensor based technique. Simulated results for sensor based and sensorless zero direct axis current control has been shown in this paper.**

**Index Terms: Zero Direct Axis Current Control (ZDAC), Permanent magnet synchronous motor (PMSM)**

## I. Introduction

The permanent-magnet synchronous motor (PMSM) is attracting attention in recent years and it is widely recognized to be a very suitable candidate for hybrid and electric vehicles' applications. Maintenance free operation, robustness against environment, high efficiency, high power density, and high controllability are some of the PMSM characteristics responsible for its wide utilization in traction applications such as electric vehicles (EVs) and hybrid EVs (HEVs). In PMSM drives, position sensors are required to time the sinusoidal current waveforms with the rotor position; suitable waveforms of phase currents and low motor torque ripple ask for high resolution sensors such as either optical encoders or electromagnetic resolvers. However, these sensors are expensive and their coupling very

often requires special constructions for the machine, such as a second shaft end; besides, position sensor misalignment can often occur during operation causing unexpected current overloads. In direct drive PMSMs which are widely used for traction applications it is required a periodic Monitoring of the sensor alignment and, if necessary, the software correction of the reference position angle. The requirement of removal of unreliable and expensive position sensors has led academic and industrial researchers to investigate and to propose several methods for the sensorless control of electrical machines. Within the last decade, significant improvements have been made in the field of sensorless control of PMSMs; major methods for sensorless position estimation can be classified in two main groups, the first group collects methods which use back-electromotive-force (EMF) estimation with fundamental excitation, whereas the second group is related to spatial saliency image tracking methods which use excitation in addition to the fundamental [1]. The saliency tracking methods are appropriate for zero and near zero-speed operation, however machines with suitable saliency are required for correctly estimate the rotor position; back-EMF-based methods are easy to be implemented for symmetric PMSMs, however the failure of these methods at low rotational speed preclude their acceptance in direct drive PMSMs for traction applications. In this paper a back-EMF-based method is used in conjunction with very low resolution sensors [2]–[5] to estimate the rotor position of direct-drive PMSMs to be used for traction purpose of an electric wheelchair. A speed estimator based on rotor frame machine model (SERF) has been implemented for the

PMSM drives, and then the rotor position estimation is achieved by means of a discrete integration of the estimated speed. During the manufacturing process three very low-cost integrated circuits based on the Hall-effect are suitably positioned in the machine stator in order to provide 60 electrical degrees resolution in rotor position sensing, thus the error on the rotor position estimation is reset every time the rotor's magnetic axes enters a new 60 sector univocally identified by means of the three Hall-effect sensors' binary code. The Hall-effect sensors do not require any tuning process and are also used to detect the initial position of the machine rotor, in this case the rotor's magnetic axes is positioned at the half of the 60 electrical sector identified by means of the sensors' binary code. As a consequence the drive is able to start in sinusoidal operation at a torque which is in the range of 86.6%–100% of the maximum torque, in fact the maximum error in the initial position detection is 30 electrical degrees and it is reset to zero at the very first transition of any of the Hall-effect sensors.

**II. Mathematical Model of PMSM**

The two axis PMSM stator windings can be considered to have equal turns per phase. The rotor flux can be assumed to be concentrated along the d-axis while there is zero flux along the q-axis, an assumption similarly made in the derivation of indirect vector-controlled induction motor drives. Further, it is assumed that the machine core losses are negligible. Also, rotor flux is assumed to be constant at a given operating point. Variations in rotor temperature alter the magnet flux, but its variation with time is considered to be negligible. There is no need to include the rotor voltage equations as in the induction motor, since there is no external source connected to the rotor magnets, and variation in the rotor flux with respect to time is negligible. When rotor reference frames are considered, it means the equivalent q and d axis stator windings are transformed to the reference frames that are revolving at rotor speed. The consequence is that there is zero speed differential between the rotor and stator magnetic fields and the stator q and d axis windings have a fixed phase relationship with the rotor magnetic axis, which is the d axis in the modeling[6].

The stator flux-linkage equations are

$$V_{qs}^r = R_q i_{qs}^r + p \lambda_{qs}^r + \omega_r \lambda_{ds}^r \quad (1.1)$$

$$V_{ds}^r = R_d i_{ds}^r + p \lambda_{ds}^r - \omega_r \lambda_{qs}^r \quad (1.2)$$

where  $R_q$  and  $R_d$  are the quadrature and direct-axis winding resistances, which are equal (and hereafter referred to as  $R_s$ ), and the q and d axes stator flux linkages in the rotor reference frames are

$$\lambda_{qs}^r = L_s i_{qs}^r + L_m i_{qr}^r \quad (1.3)$$

$$\lambda_{ds}^r = L_s i_{ds}^r + L_m i_{dr}^r \quad (1.4)$$

but the self-inductances of the stator q and d axes windings are equal to  $L_s$  only when the rotor magnets have an arc of electrical  $180^\circ$ .

The q axis current in the rotor is zero, because there is no flux along this axis in the rotor, by assumption. Then the flux linkages are written as

$$\lambda_{qs}^r = L_q i_{qs}^r \quad (1.5)$$

$$\lambda_{ds}^r = L_d i_{ds}^r + L_m i_{fr}^r \quad (1.6)$$

where  $L_m$  is the mutual inductance between the stator winding and rotor magnets.

Substituting these flux linkages into the stator voltage equations gives the stator equations:

$$\begin{bmatrix} V_{qs}^r \\ V_{ds}^r \\ \omega_r L_m i_{fr}^r \\ 0 \end{bmatrix} = \begin{bmatrix} R_q + L_q p & \omega_r L_d \\ -\omega_r L_q & R_d + L_q p \end{bmatrix} \begin{bmatrix} i_{qs}^r \\ i_{ds}^r \end{bmatrix} + \begin{bmatrix} 0 \\ 0 \\ \omega_r L_m i_{fr}^r \\ 0 \end{bmatrix} \quad (1.7)$$

The electromagnetic torque is given by

$$T_e = \frac{3P}{2} \{ \lambda_{ds}^r i_{qs}^r - \lambda_{qs}^r i_{ds}^r \} \quad (1.8)$$

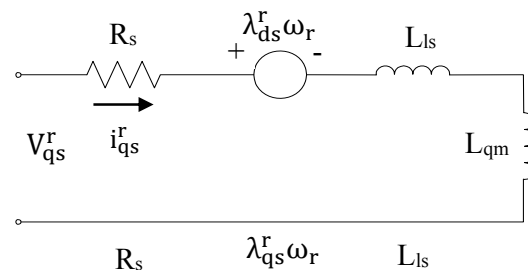
which, upon substitution of the flux linkages in terms of the inductances and currents, yields

$$T_e = \frac{3P}{2} \lambda_m i_{qs}^r + (L_d - L_q) i_{qs}^r i_{ds}^r \quad (1.9)$$

Where the rotor flux linkages that link the stator are

$$\lambda_m = L_m i_{fr}^r \quad (1.10)$$

The voltage and flux linkage equation suggest the equivalent circuit



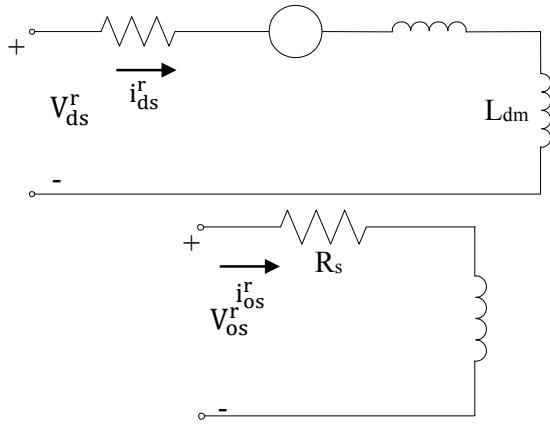


Fig.1. Equivalent circuit of PMSM in rotor reference frame

### III. Rotor Position Estimation

The rotor position can be estimated based on back electromotive force (EMF) calculated by integration of the total flux linkage on the stator phase circuits. This system is simpler but cannot assure control at standstill or at very low speed and suffers also from flux-integrator’s drift problem, particularly in the analog realization

Assuming a balanced three-phase system, the expression of the back EMF space vector  $e_s$  components is

$$e_s = v_s - Ri_s = e_{s\alpha} + je_{s\beta} \quad (1.11)$$

$$= [v_a - \frac{j}{\sqrt{3}}(v_a + 2v_b)] - R[i_a - \frac{j}{\sqrt{3}}(i_a + 2i_b)] \quad (1.12)$$

$$= v_a - Ri_a + \frac{j}{\sqrt{3}} [(v_a + 2v_b)] - R(i_a + 2i_b) \quad (1.13)$$

in which

$v_a, v_b, i_a, i_b$  respective voltages and currents of phases “A” and “B”;

$i_s$  space vector of the stator currents.

$e_{s\alpha}$  and  $e_{s\beta}$  respective components along the stationary real and imaginary axes of the back EMF space vector  $e_s$ . The argument of the back EMF clearly is not the real rotor position. The real rotor position is given by the difference between the argument of  $e_s$  in the stator reference frame and the argument of the same one in the rotating dq frame. A simple analysis on the machine model at steady state with  $i_d = 0$  gives the following expression for correct rotor position:

$$\theta = \arctan \left[ \frac{e_{s\beta}}{e_{s\alpha}} \right] - \arctan \left[ \frac{\lambda_m}{L_q i_q} \right] \quad (1.14)$$

$$\theta = \arctan \left[ \frac{v_\beta - Ri_\beta}{v_\alpha - Ri_\alpha} \right] - \arctan \left[ \frac{\lambda_m}{L_q i_q} \right] \quad (1.15)$$

where,

$\arctan \left[ \frac{e_{s\beta}}{e_{s\alpha}} \right]$  is the phase of the  $e_s$  vector in the stationary reference frame and  $\arctan \left[ \frac{\lambda_m}{L_q i_q} \right]$  (to which we refer as the “current-offset term”) is the angle of the same vector computed in the dq reference frame. Equation (1.14) presents two singularities when  $e_{s\alpha}$  or  $i_q$  approaches zero crossings. Sometimes named atan2 in the field of technical computing is a suitable alternative to the simple arctan function. Equation (1.14) gives only an early and rough estimation term to be used in the control system. In the following, it is presented how to realize a satisfactory estimation that allows controlling the drive also during transient operations [7]-[11].

### IV. Zero direct axis current control

In this control, the torque angle  $\delta$  is maintained at 90 degrees; hence, the field or direct-axis current is made to be zero, leaving only the torque or quadrature-axis current in place. This is the mode of operation for speeds lower than the base speed. Such a strategy is commonly used in many of the drive systems. [6]

The relevant equations of performance in this mode of operation are

$$T_e = \frac{3P}{2} \lambda_{af} i_{qs}^r + (L_d - L_q) i_{qs}^r i_{ds}^r \quad (1.16)$$

If the d axis current made equal to zero

$$i_{ds}^r = 0 \quad (1.17)$$

By putting this value in equation for electromagnetic torque we can get

$$T_e = \frac{3P}{2} \{ \lambda_{af} i_{qs}^r \} \quad (1.18)$$

Arranging this equation

$$i_{qs}^r = \frac{T_e}{\left(\frac{3}{2}\right) \left(\frac{P}{2}\right) \lambda_{af}} \quad (1.19)$$

Constant torque angle phasor is shown in figure 2.

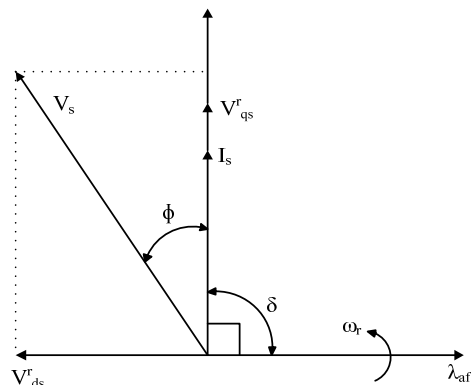


Fig.2. Constant torque-angle or Zero d-axis control phasor[6]

**V. The control algorithm for sensor based ZDAC**

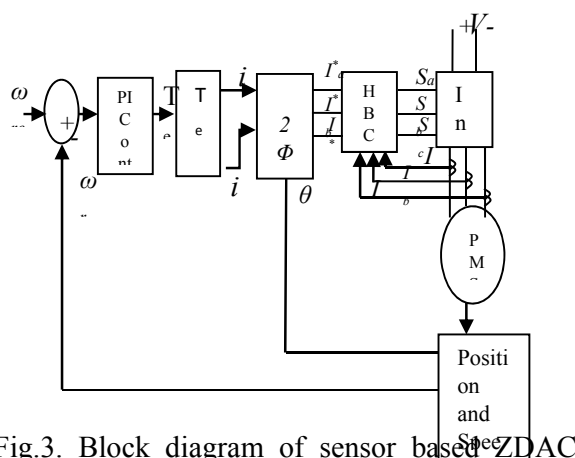


Fig.3. Block diagram of sensor based ZDAC controlled PMSM drive

**VI. The control algorithm for sensorless ZDAC**

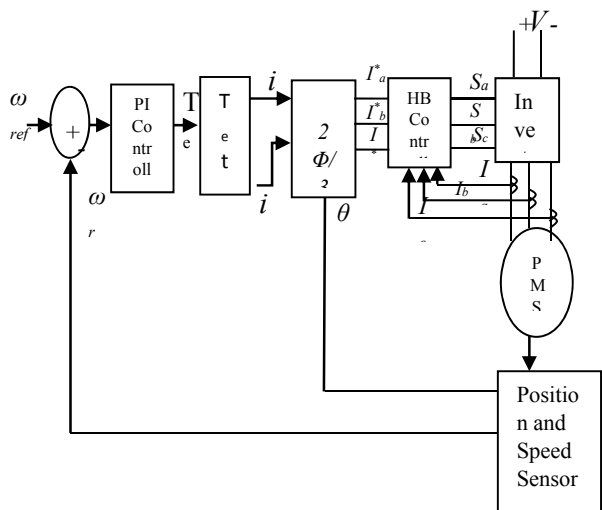


Fig.4. Block diagram of sensorless ZDAC controlled PMSM drive

**VII. Specification of simulated motor**

|                              |                             |
|------------------------------|-----------------------------|
| stator phase resistance      | 0.9585Ω                     |
| flux induced by the magnet λ | 0.1827 Wb                   |
| d-axis inductance (Ld)       | 0.004987 H                  |
| q-axis inductance (Lq)       | 0.005513 H                  |
| Moment of inertia (J)        | 0.0006329 kg-m <sup>2</sup> |
| No of poles                  | 4                           |
| Friction Constant            | 0.0003035 N-m-s             |
| Base speed                   | 1500 rpm                    |

**VIII. Simulated Results**

The simulation result for sensor based zero d axis current control at 1000 rpm speed under no load has been shown in the figure 5.

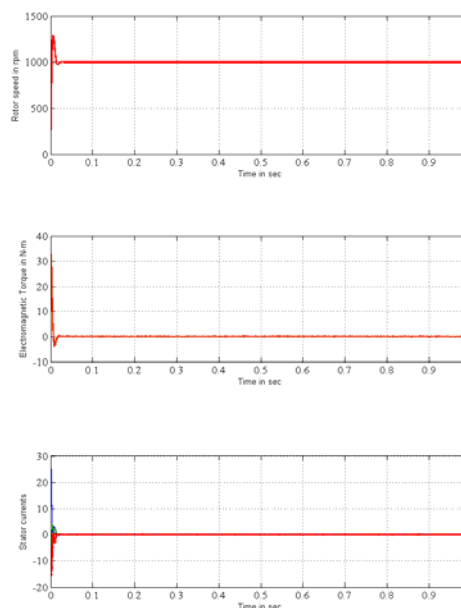
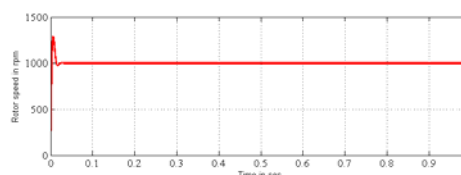


Fig.5. Simulation result of sensor based ZDAC controlled PMSM drive at 1000 rpm with no load

The simulation result for sensorless zero d axis current control at 1000 rpm speed under no load has been shown in the figure 6.



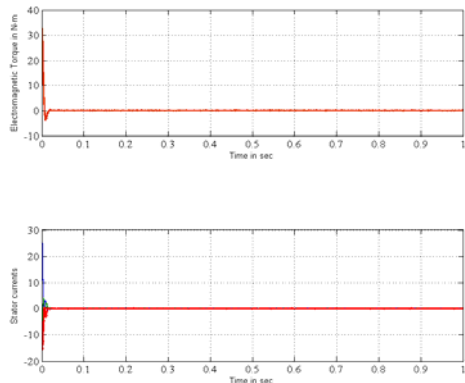


Fig.6. Simulation result of sensorless ZDAC controlled PMSM drive at 1000 rpm with no load

The simulation result for sensor based zero d axis current control at 1500 rpm reference speed under load has been shown in the figure 7.

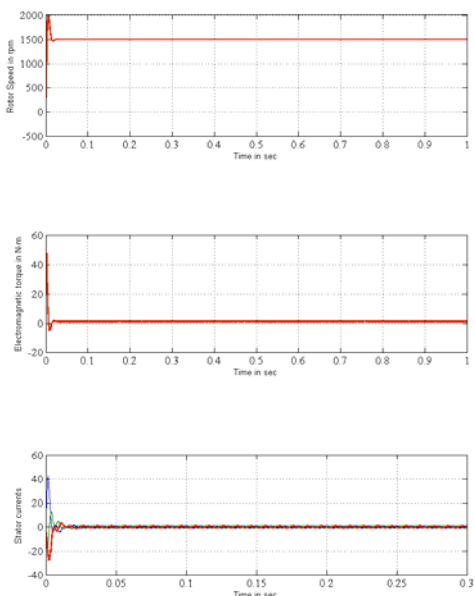


Fig.7. Simulation result of sensor based ZDAC controlled PMSM drive at 1500 rpm under load

The simulation result for sensorless zero d axis current control at 1500 rpm reference speed under load has been shown in the figure 8.

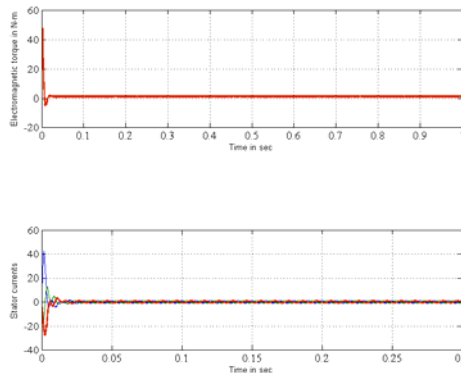
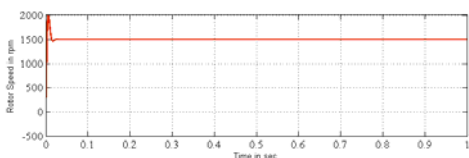


Fig.8. Simulation result of sensorless ZDAC controlled PMSM drive at 1500 rpm under load

### IX. Conclusion

The Rotor position estimation of PMSM has been done based on the back EMF space-vector estimation. The use of the back EMF space vector is advantageous with respect to any other system using flux estimation because of the integrator elimination avoiding the problem of integration drift that requires opportune devices or subsystems for its compensation. This simplification also includes that the control system will be less susceptible against the EMI external sources. The proposed system, in general, is more reliable and cheaper than a complicated one without loss of performance with respect to the other control systems proposed in literature or in industrial applications. In conclusion, the proposed algorithm may be considered a very good alternative in terms of economy and precision without lack of performances and, furthermore, exhibits an increase in reliability.

### X. References

[1] C. C. Chan, J. Z. Jiang, G. H. Chen, and X. Y. Wang, "A novel high powerdensity permanent magnet variable-speed motor," *IEEE Trans. EnergyConvers.*, vol. 8, no. 2, pp. 297–303, Jun. 1993.

[2] H. A. Toliyat, M. M. Rahimian, and T. A. Lipo, "Analysis and modeling of five phase converters for adjustable speed drive applications," in *Proc. Eur. Conf. Power Electron. and Appl.*, 1993, vol. 5, pp. 194–199.

[3] L. Parsa and H. A. Toliyat, "Multi-phase permanent magnet motor drives," in *Conf. Rec. IEEE IAS Annu. Meeting*, Salt Lake City, UT, Oct. 12–16, 2003, pp. 401–408.

- [4] L. Takahashi and T. Noguchi, "A new quick response and high efficiency strategy of induction motor," in *Conf. Rec. IEEE IAS Annu. Meeting*, 1985, pp. 495–502.
- [5] M. Depenbrock, "Direct self controlled (DSC) of inverter-fed induction machines," *IEEE Trans. Power Electron.*, vol. 3, no. 4, pp. 420–429, Oct. 1988.
- [6] Krishnan, R. "Electric Motor Drives Modeling, Analysis, and Control", *Pearson Education*, 2001.
- [7] M. Raganella, A. Di Napoli, F. Crescimbin, A. Lidozzi, and L. Solero, "Design and modeling of controllers in PM drives for wheelchairs," in *Proc. IECM'04*, 2004, [CD ROM].
- [8] H. W. van der Broeck, H. C. Skudelny, and G. V. Stanke, "Analysis and realization of a pulse width modulator based on voltage space vectors," *IEEE Trans. Ind. Appl.*, vol. IA-24, no. 1, pp. 142–150, Jan./Feb. 1988.
- [9] G. Vitale, A. Di Napoli, F. Crescimbin, A. Lidozzi, and L. Solero, "Combination of SVM techniques for electric drive," in *Proc. SPEEDAM'04*, 2004, [CD ROM].
- [10] J.-W. Choi and S.-K. Sul, "A new compensation strategy reducing voltage/current distortion in PWM VSI systems operating with low output voltages," *IEEE Trans. Ind. Appl.*, vol. 31, no. 5, pp. 1001–1008, Sep./Oct. 1995.
- [11] L. Sang-Bin, T. G. Habetler, R. G. Harley, and D. J. Gritter, "An evaluation of model-based stator resistance estimation for induction motor stator winding temperature monitoring," *IEEE Trans. Energy Conv.*, vol. 17, no. 1, pp. 7–15, Mar. 2002